THE JOURNAL OF PHYSICAL CHEMISTRY LETTERS
A JOURNAL OF THE AMERICAN CHEMICAL SOCIETY

pubs.acs.org/JPCL

Letter

Strong Enhancement of Nanoconfined Water Mobility by a Structure Breaking Salt

Naresh C. Osti,* Bishnu Prasad Thapaliya, Sheng Dai, Madhusudan Tyagi, and Eugene Mamontov*

Cite This: J. Phys. Chem. Lett. 2021, 12, 4038−4044

Read Online

ACCESS | Metrics & More | Article Recommendations | Supporting Information

ABSTRACT: For the majority of the water present on earth, the two most important factors influencing its behavior are confinement, in either inorganic or organic matrixes, and the presence of solutes. Here, we investigate the effect of confinement in 3 nm pores on water diffusivity in aqueous solutions with archetypical solutes, a structure making (kosmotrope) NaCl and a structure breaking (chaotrope) KCl, up to 1.0 M in concentration. The water diffusivity in bulk aqueous solutions in such a concentration range is known to decrease very slightly in the presence of NaCl and increase very slightly in the presence of KCl. However, here we observe the water diffusivity in confined H_2O−KCl increases by a factor of 2 compared to the pure water diffusivity in the same confinement. This unusually strong cumulative effect of confinement and a structure breaking additive may have profound implications for the mobility and transport of aqueous species in nature.

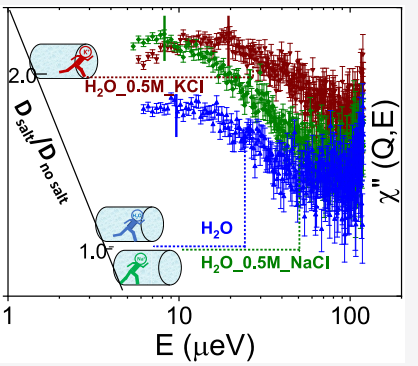

As a ubiquitous and versatile solvent, water is often found in solutions and confined environments. Physicochemical properties of water in bulk, confined in various media, or in solutions are dramatically different.[1−3] These properties are critical for the performance of materials in applications, such as energy storage in electrical double-layer capacitors,[4−6] as well as for the ion transport in biological[7,8] and synthetic membranes.[9−12] Ion transport and electrochemical activities in energy storage devices are closely related to the structure and dynamics of confined hydrated ions. The strength and the number of molecules in a hydration shell, which is an envelope of water molecules formed around an ion during solvation, depends on the nature of the solvated ions.[13,14] It has been well demonstrated that the size of ions together with the electron densities on the surface of ions control the ion−water interactions, thereby impacting the mobility of water molecules.[15,16] Even in the absence of ions, water in confinement exhibits substantially varied characteristics, depending on the shape, size, and surfaces of the confining matrixes.[17,18] When water is confined together with metal ions, the structure and dynamics of water are impacted by not only the nature of metal ions but also the morphology of the confining media.[19−21]

The mobility of water in different aqueous salt solutions has been a target of many investigations to explore the microscopic dynamics, as well as to relate them to various technological and biological processes. In particular, the behavior of two alkali metal ions, Na^+ and K^+, in their aqueous solutions has been studied extensively by both experiments and simulations.[13,22,23] These studies revealed formation of a relatively tight hydration shell by the Na^+ ion compared to the K^+ ion, which are classified as kosmotrope (structure making) and chaotrope (structure breaking), respectively. Furthermore, the existence of the second hydration shell around these ions has also been confirmed.[24,25] The structure of those hydration shells determines the viscosity of aqueous salt solutions[26,27] and impacts the water diffusivity. Using the quasi-elastic neutron scattering (QENS) technique, Ishai et al.[28] studied the dynamics of water in aqueous solutions of NaCl and KCl. They observed a slowing down of water mobility in NaCl solution, but an enhancement in the diffusivity of water in KCl solution. There was a strong concentration effect on the diffusion coefficient of water in NaCl solution, but only a weak effect, to a certain concentration range, in KCl solution. Those observations were rationalized on the basis of the structure making and structure breaking nature of Na^+ and K^+ ions with water molecules. It was concluded that the structure making effect is cumulative and, therefore, a function of concentration. In contrast, the structure breaking effect is not cumulative, hence almost the concentration-independent diffusion coefficient of water in KCl solutions. The dynamics of water in aqueous salt solutions in confinement has also been studied using QENS. Mamontov et al.[29] explored the dynamics of water in the aqueous solution of LiCl and $CaCl_2$ confined in silica matrixes of different pore sizes. They reported a bulk water-like behavior in the aqueous solutions confined in larger

Received: February 9, 2021
Accepted: April 12, 2021

https://doi.org/10.1021/acs.jpclett.1c00461
J. Phys. Chem. Lett. 2021, 12, 4038−4044

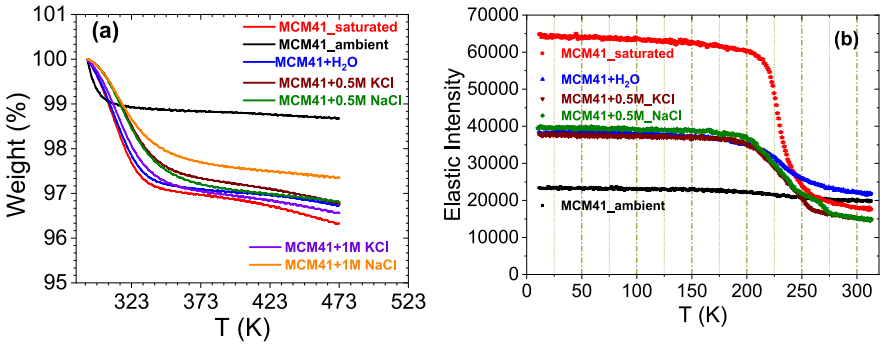

Figure 1. (a) Thermogravimetric analysis curves showing changes in weight of the samples on increasing the temperature. (b) Elastic neutron scattering intensities as a function of temperature

pores. However, a clear impact of confinement was observed in smaller pores. Furthermore, they reported a significant reduction of water mobility in the aqueous solution of $CaCl_2$ in confinement due to a combined effect of confinement and higher charge density of calcium ion compared to lithium ion. Recently, Baum et al.[30] investigated the dynamics of water molecules in aqueous solutions of three different chloride salts comprising three kosmotropic ions (Ba^{2+}, Ca^{2+}, and Mg^{2+}) in mesoporous silica of variable pore sizes using QENS. Along with other observations, they found an optimum pore size of the matrixes and a concentration of those salts at which the dynamics of water molecules is independent of the salt concentration but depends only on the pore size. Even though there are studies on the structure and dynamics of water of aqueous salt solutions in bulk[28] and in confinement,[20,29−32] a straight comparison of the dynamics of water in aqueous solutions with distinctively chaotropic and distinctively kosmotropic ions in confinement has never been attempted (e.g., all the cations studied in refs 30−32 were, to varying degree, kosmotropic). Here we explore the dynamics of water in aqueous solutions of NaCl and KCl of various concentrations confined in MCM41 mesoporous silica. As a reference, we have also made a comparison with pure water confined in MCM41 by employing different sample hydration procedures. We find that the mobility of water in the confined aqueous solution is significantly reduced compared to the values reported for the bulk aqueous solutions.[28] The concentration dependent diffusivity of the water in aqueous solution of NaCl follows an opposite trend compared to their bulk solutions[28] due to phase separation. Most remarkably, the diffusion coefficient of water is almost twice as large in confined KCl solution than in pure water and NaCl solution in the same confinement, showing the much-enhanced impact of the structure breaking vs structure making properties in confinement compared to that in the bulk state.

Accurate depiction of the aqueous system in confinement critically depends on the characterization of the confining matrix. Brunauer−Emmett−Teller (BET) derived surface area (Figure S1a) and the pore volume of the dry MCM41 are 698.1 and 0.535 $cm^3\ g^{-1}$, respectively. Pore-size distribution (Figure S1b) obtained by using density functional theory indicates the presence of both micro- and mesopores in the dry MCM41, with a majority of pores of ca. 3 nm (Figure S1b, inset) in size. Dry MCM41 samples (Table T1 in the Supporting Information) treated with pure and aqueous salt solutions (see the Supporting Information for sample preparation details) were characterized by TGA, which shows a variable amount of weight loss. The amount of water within the pores in relation to the porous volume of the MCM41_dry is presented in the Supporting Information (Table T2). Note that the TGA measurements were carried out up to 200 °C under ambient air, which could not remove all the confined water. Therefore, we calculated the volume of the pores occupied based on the weight difference between the wet (samples listed in Table T1 of the Supporting Information) and the corresponding dry MCM41 samples before loading. TGA curves (Figure 1a) show that MCM41-ambient loses less than 1% mass. The highest weight loss is from the MCM41_saturated sample. The rest of the samples exhibit roughly the same amount (2−3 wt %) of weight loss. The weight loss obtained from TGA correlates with the amount of water present in those samples, which was further confirmed from the elastic neutron scattering measurements (details in the Supporting Information). As presented in Figure 1b, the elastic intensity at 20 K from MCM41_saturated sample is the highest among them. This indicates that MCM41_saturated, as already seen from the TGA curve, holds a higher amount of water. Similarly, the elastic intensity at 20 K from the MCM41-ambient is the lowest, indicating only traces of water. The elastic intensities at 20 K from other samples lay between the intensities from the MCM41_saturated and the MCM41_ambient samples and are remarkably close among the three similarly prepared samples of primary interest, indicating practically the same amount of water in them.

Besides the MCM41_ambient, all other samples show a decrease in the elastic intensities in the temperature range of 200−250 K, demonstrating the onset of the measurable diffusion of water molecules in them. Such temperature dependences are evident both on heating and cooling curves (Figures S2). The presence of a minimal amount of water in the MCM41_ambient sample gives rise to a tiny step in the elastic scan. The sharp drop in the elastic intensity in MCM41_saturated around 230 K is due to the increased mobility of water in confinement. Since the amount of water present in this sample is significantly higher than other samples, the transition looks more pronounced. A similar type of transition in elastic intensity scans has been observed for water confined in MCM41.[29] Other samples also show the transition but very gradually. Studies of various confined water systems have proven such transition of confined water predominantly depends on the size of confinement.[33,34] Since the matrix is the same, the differences in the elastic intensities among MCM41_saturated, MCM41_ambient, and MCM41+H_2O samples can be related to the amount of water present inside the samples. However, effects on MCM41_0.5

https://doi.org/10.1021/acs.jpclett.1c00461
J. Phys. Chem. Lett. 2021, 12, 4038−4044

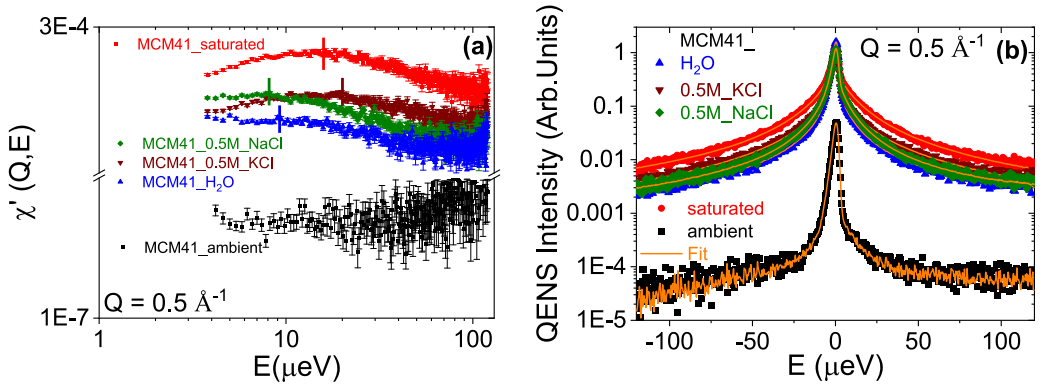

Figure 2. Dynamic susceptibility curves (a) generated from the corresponding QENS data (b) at $Q = 0.5$ A^{-1}, and $T = 285$ K. The vertical lines on the curves in the figure correspond to the peak's maxima. Solid lines in (b) are the fits obtained using the model function described in the text.

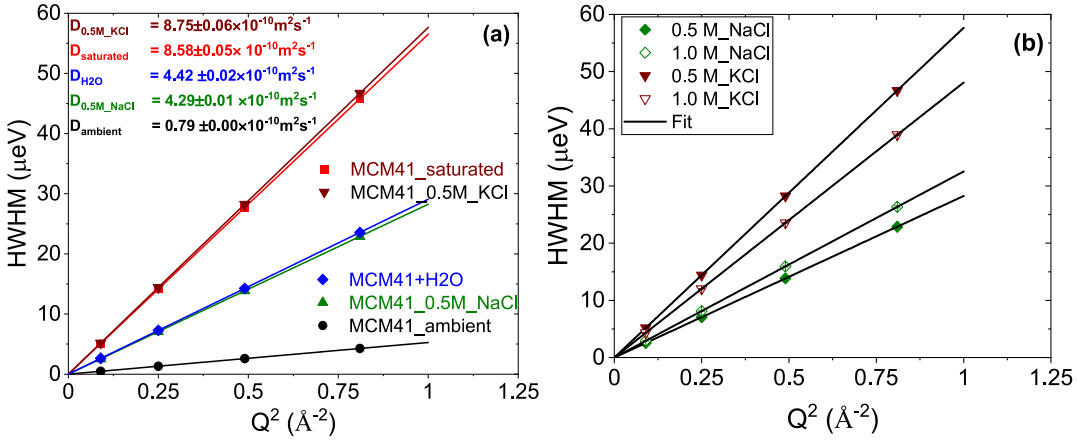

Figure 3. (a) Dependence of HWHM of the QENS spectra with the square of the momentum transfer illustrating a linear relationship. (b) shows an impact of concentration on the HWHM.

M_NaCl and MCM41_0.5 M_KCl can be attributed primarily to the presence of Na^+ and K^+ ions, given a similar amount of water in these three samples.

MCM41 with confined aqueous salt solutions exhibit similar elastic scan patterns collected on heating except for the presence of a kink around 265 K in aqueous NaCl solutions at both concentrations (Figure S3-I). This bend on the elastic scan can be attributed to a possible phase separation of the aqueous solution of NaCl, likely due to the formation of dihydrate salt,[35] in confinement. A similar nature of the kink observed in the elastic scan of aqueous $CaCl_2$ confined in MCM41 was assigned for a phase transition in a phase-separated system.[29]

QENS measurements were performed to probe the diffusion dynamics of water molecules in pure and aqueous salt solutions confined in MCM41. QENS signal predominantly depends on the incoherent neutron scattering cross section of an atom.[36] Since hydrogen has the highest incoherent scattering cross-section, the QENS spectra in our measurements predominantly represent the mobility of water molecules. Figure 2a shows an imaginary part of dynamic susceptibility, $\chi''(Q, E)$, obtained from the measured QENS data as $\chi''(Q, E) = \frac{I(Q,E)}{n_{\text{Bose}}(E)+1}$, where $n_{\text{Bose}}(E)$ is Bose population factor and is given by $\left(\exp\left(\frac{E}{k_B T}\right) - 1\right)^{-1}$. Note that maxima of the dynamic susceptibility correspond to the energy (time) scale of the relaxation processes, and the number of such visible peaks identifies the number of different dynamic processes measurable in the system.[37] The dynamic susceptibilities show a single broad peak with different peak maxima in all the samples except in MCM41_ambient, where the peak is not well-defined. However, all the spectra could be fitted with a single Lorentzian function. The QENS spectra together with the model fit (see the Supporting Information for details) are presented in Figure 2b. There is a noticeable shift of the peak position of the susceptibility curves (Figure 2a) to the higher energy transfer in the MCM41_0.5 M_KCl.

Half-width at half-maxima (HWHM) of the $S(Q,E)$ spectra obtained from the model fit (see the Supporting Information for detail) shows a strong Q-dependence (Figure 3a,b) suggesting a long-range translational diffusion process of water molecules in those samples. A linear fit of HWHMs with Q^2 provided the diffusion coefficients (see the Supporting Information for details) of water molecules. As suggested from the elastic scan and TGA, the diffusivity of water in the MCM41_ambient sample is very small, $0.79 \pm 0.00 \times 10^{-10}$ m^2 s^{-1}, compared to $8.58 \pm 0.05 \times 10^{-10}$ m^2 s^{-1} obtained for the MCM41_saturated sample. It is well recognized that the hydration level of pores significantly affects the translational diffusion coefficient in confined water.[17,38,39] The lower value of diffusivity in the MCM41_abmient sample is due to the very minimal amount of water present in this sample, where most of the water molecules are attached to, or influenced by, the wall. Therefore, QENS analysis shows a higher value (Figure S5) of

https://doi.org/10.1021/acs.jpclett.1c00461
J. Phys. Chem. Lett. 2021, 12, 4038−4044

elastic incoherent scattering factor (EISF) and a lower value of the diffusion coefficient. On the other hand, MCM41_saturated sample hydrated to the highest level shows a lower value of EISF but a higher diffusion coefficient due to an impact of hydration on the translational diffusivity of water molecules. Even though the amounts of water in MCM41+H_2O, MCM41_0.5M_NaCl, and MCM41+0.5M_KCl are almost the same, as evidenced by Figure 1, EISF from MCM41+H_2O is the highest among them, meaning that most of the water molecules in this sample are influenced by the pore wall. However, the EISFs from MCM41_0.5M_NaCl and MCM4+0.5M_KCl are roughly the same, but the diffusion coefficient is 2 times higher in confined 0.5 M KCl salt solution. This observation illustrates that, with all other parameters virtually identical, the structure breaking characteristics of K^+ ion disturb the hydrogen bonding network of the confined water molecules significantly, which results in substantially increased water diffusivity. The much-increased diffusivity value is corroborated by the position of the susceptibility peak (right shift of the peak position as indicated by a solid line in Figure 2a), proving that the effect is model-independent. The tendency of Na^+ ion to form a tight hydration shell around it lowers the average diffusivity value of water in confinement to $4.29 \pm 0.01 \times 10^{-10}$ m^2 s^{-1}.

The effect of concentration on the dynamics of water in both confined salt solutions is reflected in both elastic and QENS spectra (see the Supporting Information, Figures S3 and S4). HWHM and the diffusivity of water in confined aqueous salt solutions extracted after the analysis are presented in Figures 3b and 4, respectively. The diffusion coefficients as a function

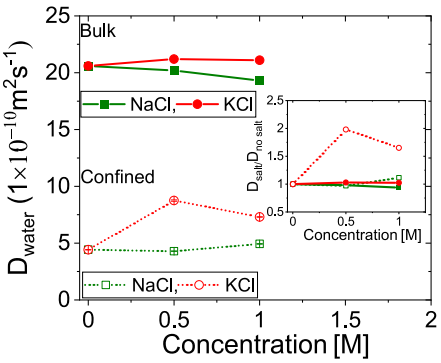

Figure 4. Impact of concentration on diffusivities where water diffusivities in bulk aqueous solutions extracted from the Ishai et al.[28] paper are also shown. The inset in the figure represents the ratio of diffusivities from bulk aqueous and confined aqueous solutions to the corresponding diffusivity values at zero salt concentration. The error bars in the figure are within the symbols.

of concentration (Figure 4) were obtained from the linear dependence of HWHM with Q^2 (Figure 3b). Similar to the bulk aqueous salt solutions (Figure 4), there is an increase in the average diffusion coefficient of water for KCl and a decrease in the diffusion coefficient for NaCl solution at a concentration of 0.5 M. Likewise, a small increase in the diffusivity in the presence of KCl has also been observed in the aqueous 1-propanal solution.[40] At 1 M concentration, the diffusion coefficient for the KCl solution is still higher compared to the diffusivity at zero salt concertation, but lower than the value obtained in 0.5 M solution. This slight decrease in the average diffusion coefficient could be a limiting case because of an absence of contact pair (between K^+ and Cl^-) and hydration shell formation by K^+ ion in the solution at a higher concentration. This observation is consistent with the leveling off of the diffusion coefficient values at higher concentrations reported for bulk KCl solutions.[28] However, there is roughly a 2-fold increase, as indicated from the ratio of diffusivities from bulk aqueous and confined aqueous solutions to the corresponding diffusivities values at zero salt concentration (inset in Figure 4), in the diffusivity of water molecules in the confined KCl solution compared to the bulk solution, which we attribute to the cumulative effect of confinement and the water-structure breaking nature of the K^+ ion. Interestingly, contrary to the observations made for the bulk NaCl solutions as a function of concentration, we found an increase in the diffusivity of water molecules in the confined 1 M NaCl solution. In general, an increase in the concentration of a kosmotropic ion results in more water molecules in its hydration shell that lowers the average diffusion coefficient of the water molecules. However, we believe that this general mechanism of the water structure making process does not take place in the confined 1 M NaCl solution. Elastic intensity scans (Figure 1b and Figure S2-IV) of 0.5 and 1 M NaCl solutions in confinement show a clear indication of phase separation. An increase in the average diffusivity of water in confined 1 M NaCl solution can be attributed to this phase separation. Not only at the higher concentration but also at a concentration of 0.5 M is the decrease in the diffusivity value small compared to the trend reported for the bulk solutions. This means that, when aqueous NaCl solutions are confined, their structure making property is somehow compromised in MCM41, and therefore, an opposite trend compared to bulk on diffusivity is observed. To understand the behavior of the aqueous solution of NaCl in confinement and investigate the observed phase transition and the underlying physics of Na^+ ions and water molecules' interaction with the wall of the confined matrix, a thorough study in future is required.

However, some questions regarding the origin of the unusual behavior of confined water in the presence of KCl can be addressed on the basis of the discussion by Baum et al.[30] Specifically, we contend that the large increase in the water diffusivity cannot be explained singularly from the chaotropic influence of the potassium ions, but must be largely due to the influence of the interfacial layer near the pore walls. This is evident from examination of the concentration dependence of water diffusivity in bulk KCl solutions,[24] where the increase in the diffusivity compared to pure water, evident within the limited concentration range, always remains small. That is, no matter what the concentration of KCl solution in the middle of the pore is, it cannot be responsible for the observed nearly 2-fold increase in the confined water diffusivity. According to Baum et al.,[30] the pore size of 3.0 nm with Mg^{2+}, Ca^{2+}, and Ba^{2+} in our concentration range would represent a borderline case between the larger pores, where the dominant effect on the confined water dynamics would be predominantly due to the kosmotropic/chaotropic character of the ions, and the smaller pores, where the confinement itself would exert the major influence on the water dynamics. In our case, with Na^+ ions, similar consideration should apply, as the hydration shell size for kosmotropic Na^+ ions is only slightly larger compared to those for Mg^{2+}, Ca^{2+}, and Ba^{2+}. On the other hand, despite its nominally larger hydration shell, chaotropic K^+ can readily shed it, e.g., when it goes through the narrow biomembrane potassium channels.[41] This situation of a small enthalpic

https://doi.org/10.1021/acs.jpclett.1c00461
J. Phys. Chem. Lett. 2021, 12, 4038−4044

penalty for shedding the hydration shell is equally applicable to the potassium adsorptions on the pore walls. Without its hydration shell, the size of the K^+ cation is rather small. That is, the solution in the middle of the pores effectively experiences weaker confinement than a solution in the similar pores, but with ions adsorbed on the walls with their hydration shell. At a first glance, this makes the situation with K^+ adsorbed in the interfacial layer qualitatively similar to that encountered in the pores larger than the borderline value of 2.9 nm,[30] where the ions in the solution in the middle of the pore, not the confinement, would have the dominant influence on the water diffusivity. Yet, as we have mentioned above, there is simply no concentration of KCl that could have increased the water diffusivity by nearly a factor of 2. This suggests that the observed increase in the water diffusivity is more akin to lubrication by the interfacial layer and has no analogy with the previously studied kosmotropic ions that cannot "lubricate" the solution in the middle of the pores because they retain their hydration shells upon adsorption on the pore walls. Because the interfacial layer is represented mostly by the ions, there is only a limited contribution of the few "slow" water molecules in the interfacial layer to the overall measured diffusivity. The measured diffusivity thus reflects the motion of most of the water molecules in the pores, which is unusually fast, facilitated not so much by the potassium ions in the solution but by the potassium ions adsorbed on the pore walls.

In summary, we investigated the dynamics of water in aqueous solutions of chaotropic and kosmotropic ions confined in MCM41 using elastic and quasielastic neutron scattering. There is a significant reduction of the averaged diffusion coefficient of water of aqueous salts solutions in confinement compared to that in the bulk solutions. Even in confinement, we found an increase in mobility of water in KCl solution and a decrease in NaCl solution, qualitatively similar to the behavior of the bulk aqueous solutions. This observation suggests that the structure making and breaking properties of Na^+ and K^+ ions still manifest themselves in confinement. On increasing the concentration of aqueous NaCl in confinement, we found an increase in the diffusion coefficient of water. This behavior is opposite to the trend observed for the bulk NaCl solutions, which we attribute to the phase transition seen in the elastic scans. Most remarkably, the KCl solutions experience a cumulative impact of the confinement and the presence of K^+ ions, resulting in a 2-fold increase in water diffusivity compared to pure water, or water with Na^+, in the same confinement. Such a large increase in the water diffusivity, evident in the model-independent raw experimental data, should have important transport implications through the ion channels in biological membranes.

METHODS

Thermogravimetric analysis (TGA) was carried out on a TGA Q50 analyzer under nitrogen flow. Brunauer–Emmett–Teller (BET) method was used to calculate the surface area. Pore-size distribution was analyzed using density functional theory.

High–flux backscattering spectrometer (HFBS)[42] at the National Institute of Standards and Technology (NIST) Center for Neutron Research was used to carry out measurements of the elastically scattered neutron intensity by operating the instrument in fixed-window mode. Elastically scattered neutron intensity from 0.5 mm thick samples of ~0.35 g in flat plate aluminum holder was collected as a function of temperature on heating. Elastic intensity from each detector in the range of 0.25 $Å^{-1}$ to 1.75 $Å^{-1}$ was added to obtain the total intensity using DAVE[43] analysis software.

QENS measurements were carried out at the Oak Ridge National Laboratory, Spallation Neutron Source using Backscattering Silicon Spectrometer (BASIS).[44] BASIS provides a fine resolution of 3.7 μeV (full width at half-maximum) in the standard instrument configuration. In this configuration, an energy transfer range of ±100 μeV and a Q (momentum transfer vector) range of 0.2–2.0 $Å^{-1}$ is accessed by using a bandwidth of incoming neutrons centered at 6.4 Å. QENS data were collected at 20 K (for the sample-specific instrument resolution) and 285 K. Data were reduced using MantidPlot[45] and analyzed by QClimax[46] software. Temperatures at both the instruments were controlled by closed-cycle refrigerators.

ASSOCIATED CONTENT

Supporting Information

The Supporting Information is available free of charge at https://pubs.acs.org/doi/10.1021/acs.jpclett.1c00461.

Experimental details, tables of different forms of MCM41 studied and of the water volume in the pores, TGA and BET measurements, N_2 sorption isotherms, QENS data analysis, more elastic and QENS data (PDF)

AUTHOR INFORMATION

Corresponding Authors

Naresh C. Osti − *Neutron Scattering Division, Oak Ridge National Laboratory, Oak Ridge, Tennessee 37831, United States;* orcid.org/0000-0002-0213-2299; Email: ostinc@ornl.gov

Eugene Mamontov − *Neutron Scattering Division, Oak Ridge National Laboratory, Oak Ridge, Tennessee 37831, United States;* orcid.org/0000-0002-5684-2675; Email: mamontove@ornl.gov

Authors

Bishnu Prasad Thapaliya − *Chemical Science Division, Oak Ridge National Laboratory, Oak Ridge, Tennessee 37831, United States; Department of Chemistry, University of Tennessee, Knoxville, Tennessee 37916, United States;* orcid.org/0000-0002-1697-0509

Sheng Dai − *Chemical Science Division, Oak Ridge National Laboratory, Oak Ridge, Tennessee 37831, United States; Department of Chemistry, University of Tennessee, Knoxville, Tennessee 37916, United States;* orcid.org/0000-0002-8046-3931

Madhusudan Tyagi − *NIST Center for Neutron Research, National Institute of Standards and Technology, Gaithersburg, Maryland 20899, United States; Department of Materials Science, University of Maryland, College Park, Maryland 20742, United States*

Complete contact information is available at: https://pubs.acs.org/10.1021/acs.jpclett.1c00461

Notes

The authors declare no competing financial interest.

ACKNOWLEDGMENTS

This work was supported as part of the Fluid Interface Reactions, Structures and Transport (FIRST) Center, an Energy Frontier Research Center funded by the U.S. Department of Energy, Office of Science, Office of Basic

Energy Sciences. Work at ORNL's Spallation Neutron Source was sponsored by the Scientific User Facilities Division, Office of Basic Energy Sciences, U.S. Department of Energy. Oak Ridge National Laboratory is managed by UT-Battelle, LLC, for U.S. DOE under Contract No. DEAC05-00OR22725. QClimax is a part of the Integrated Computational Environment Modeling and Analysis of Neutron Data (ICE-MAN) (LDRD 8237) project, funded by the Laboratory Directed Research and Development program at ORNL. Access to the HFBS was provided by the center of High Resolution Neutron Scattering, a partnership between the NIST and the National Science Foundation under Agreement No. DMR-1508249. Certain commercial material suppliers are identified in this paper to foster understanding. Such identification does not imply recommendation or endorsement by the National Institute of Standards and Technology nor does it imply that the materials or equipment identified are necessarily the best available for the purpose.

REFERENCES

(1) Gallo, P.; et al. Water: A Tale of Two Liquids. *Chem. Rev.* **2016**, *116*, 7463−7500.
(2) Fayer, M. D.; Levinger, N. E. Analysis of Water in Confined Geometries and at Interfaces. *Annu. Rev. Anal. Chem.* **2010**, *3*, 89−107.
(3) Chakraborty, S.; Kumar, H.; Dasgupta, C.; Maiti, P. K. Confined Water: Structure, Dynamics, and Thermodynamics. *Acc. Chem. Res.* **2017**, *50*, 2139−2146.
(4) Mitchell, J. B.; Geise, N. R.; Paterson, A. R.; Osti, N. C.; Sun, Y.; Fleischmann, S.; Zhang, R.; Madsen, L. A.; Toney, M. F.; Jiang, D.; et al. Confined Interlayer Water Promotes Structural Stability for High-Rate Electrochemical Proton Intercalation in Tungsten Oxide Hydrates. *ACS Energy Lett.* **2019**, *4*, 2805−2812.
(5) Liang, T. T.; Hou, R. L.; Dou, Q. Y.; Zhang, H. Z.; Yan, X. B. The Applications of Water-in-Salt Electrolytes in Electrochemical Energy Storage Devices. *Adv. Funct. Mater.* **2021**, *31*, 2006749.
(6) Popov, I.; Sacci, R. L.; Sanders, N. C.; Matsumoto, R. A.; Thompson, M. W.; Osti, N. C.; Kobayashi, T.; Tyagi, M.; Mamontov, E.; Pruski, M.; et al. Critical Role of Anion-Solvent Interactions for Dynamics of Solvent-in-Salt Solutions. *J. Phys. Chem. C* **2020**, *124*, 8457−8466.
(7) Agmon, N.; Bakker, H. J.; Campen, R. K.; Henchman, R. H.; Pohl, P.; Roke, S.; Thamer, M.; Hassanali, A. Protons and Hydroxide Ions in Aqueous Systems. *Chem. Rev.* **2016**, *116*, 7642−7672.
(8) Wiggins, P. M. Role of Water in Some Biological Processes. *Microbiol. Rev.* **1990**, *54*, 432−449.
(9) Garnier, L.; Szymczyk, A.; Malfreyt, P.; Ghoufi, A. Physics Behind Water Transport through Nanoporous Boron Nitride and Graphene. *J. Phys. Chem. Lett.* **2016**, *7*, 3371−3376.
(10) Tocci, G.; Joly, L.; Michaelides, A. Friction of Water on Graphene and Hexagonal Boron Nitride from Ab Initio Methods: Very Different Slippage Despite Very Similar Interface Structures. *Nano Lett.* **2014**, *14*, 6872−6877.
(11) Renou, R.; Ghoufi, A.; Szymczyk, A.; Zhu, H.; Neyt, J. C.; Malfreyt, P. Nanoconfined Electrolyte Solutions in Porous Hydrophilic Silica Membranes. *J. Phys. Chem. C* **2013**, *117*, 11017−11027.
(12) Holt, J. K.; Park, H. G.; Wang, Y. M.; Stadermann, M.; Artyukhin, A. B.; Grigoropoulos, C. P.; Noy, A.; Bakajin, O. Fast Mass Transport through Sub-2-Nanometer Carbon Nanotubes. *Science* **2006**, *312*, 1034−1037.
(13) Marcus, Y. Effect of Ions on the Structure of Water: Structure Making and Breaking. *Chem. Rev.* **2009**, *109*, 1346−1370.
(14) Mahler, J.; Persson, I. A Study of the Hydration of the Alkali Metal Ions in Aqueous Solution. *Inorg. Chem.* **2012**, *51*, 425−438.
(15) Howard, J. J.; Perkyns, J. S.; Pettitt, B. M. The Behavior of Ions near a Charged Wall-Dependence on Ion Size, Concentration, and Surface Charge. *J. Phys. Chem. B* **2010**, *114*, 6074−6083.
(16) Rigo, E.; Dong, Z. X.; Park, J. H.; Kennedy, E.; Hokmabadi, M.; Almonte-Garcia, L.; Ding, L.; Aluru, N.; Timp, G. Measurements of the Size and Correlations between Ions Using an Electrolytic Point Contact. *Nat. Commun.* **2019**, *10*, 2382−13.
(17) Osti, N. C.; Cote, A.; Mamontov, E.; Ramirez-Cuesta, A.; Wesolowski, D. J.; Diallo, S. O. Characteristic Features of Water Dynamics in Restricted Geometries Investigated with Quasi- Elastic Neutron Scattering. *Chem. Phys.* **2016**, *465-466*, 1−8.
(18) Briman, I. M.; Rebiscoul, D.; Diat, O.; Zanotti, J. M.; Jollivet, P.; Barboux, P.; Gin, S. Impact of Pore Size and Pore Surface Composition on the Dynamics of Confined Water in Highly Ordered Porous Silica. *J. Phys. Chem. C* **2012**, *116*, 7021−7028.
(19) Muckley, E. S.; Naguib, M.; Wang, H.; Vlcek, L.; Osti, N. C.; Sacci, R. L.; Sang, X.; Unocic, R. R.; Xie, Y.; Tyagi, M.; et al. Multimodality of Structural, Electrical, and Gravimetric Responses of Intercalated Mxenes to Water. *ACS Nano* **2017**, *11*, 11118−11126.
(20) Schneider, S.; Saeckel, C.; Brodrecht, M.; Breitzke, H.; Buntkowsky, G.; Vogel, M. NMR Studies on the Influence of Silica Confinements on Local and Diffusive Dynamics in Licl Aqueous Solutions Approaching Their Glass Transitions. *J. Chem. Phys.* **2020**, *153*, 244501−13.
(21) Martinez Casillas, D. C.; Longinotti, M. P.; Bruno, M. M.; Vaca Chavez, F.; Acosta, R. H.; Corti, H. R. Diffusion of Water and Electrolytes in Mesoporous Silica with a Wide Range of Pore Sizes. *J. Phys. Chem. C* **2018**, *122*, 3638−3647.
(22) Impey, R. W.; Madden, P. A.; McDonald, I. R. Hydration and Mobility of Ions in Solution. *J. Phys. Chem.* **1983**, *87*, 5071−5083.
(23) Koneshan, S.; Rasaiah, J. C.; Lynden-Bell, R. M.; Lee, S. H. Solvent Structure, Dynamics, and Ion Mobility in Aqueous Solutions at 25 Degrees C. *J. Phys. Chem. B* **1998**, *102*, 4193−4204.
(24) Duignan, T. T.; Schenter, G. K.; Fulton, J. L.; Huthwelker, T.; Balasubramanian, M.; Galib, M.; Baer, M. D.; Wilhelm, J.; Hutter, J.; Ben, M. D.; et al. Quantifying the Hydration Structure of Sodium and Potassium Ions: Taking Additional Steps on Jacob's Ladder. *Phys. Chem. Chem. Phys.* **2020**, *22*, 10641−10652.
(25) Mancinelli, R.; Botti, A.; Bruni, F.; Ricci, M. A.; Soper, A. K. Hydration of Sodium, Potassium, and Chloride Ions in Solution and the Concept of Structure Maker/Breaker. *J. Phys. Chem. B* **2007**, *111*, 13570−13577.
(26) Jenkins, H. D. B.; Marcus, Y. Viscosity B-Coefficients of Ions in Solution. *Chem. Rev.* **1995**, *95*, 2695−2724.
(27) Luo, P.; Zhai, Y.; Senses, E.; Mamontov, E.; Xu, G.; Z, Y.; Faraone, A. Influence of Kosmotrope and Chaotrope Salts on Water Structural Relaxation. *J. Phys. Chem. Lett.* **2020**, *11*, 8970−8975.
(28) Ben Ishai, P.; Mamontov, E.; Nickels, J. D.; Sokolov, A. P. Influence of Ions on Water Diffusion-a Neutron Scattering Study. *J. Phys. Chem. B* **2013**, *117*, 7724−7728.
(29) Mamontov, E.; Cole, D. R.; Dai, S.; Pawel, M. D.; Liang, C. D.; Jenkins, T.; Gasparovic, G.; Kintzel, E. Dynamics of Water in LiCl and $CaCl_2$ Aqueous Solutions Confined in Silica Matrices: A Backscattering Neutron Spectroscopy Study. *Chem. Phys.* **2008**, *352*, 117−124.
(30) Baum, M.; Rieutord, F.; Jurany, F.; Rey, C.; Rebiscoul, D. Dynamical and Structural Properties of Water in Silica Nanoconfinement: Impact of Pore Size, Ion Nature, and Electrolyte Concentration. *Langmuir* **2019**, *35*, 10780−10794.
(31) Baum, M.; Rebiscoul, D.; Juranyi, F.; Rieutord, F. Structural and Dynamical Properties of Water Confined in Highly Ordered Mesoporous Silica in the Presence of Electrolytes. *J. Phys. Chem. C* **2018**, *122*, 19857−19868.
(32) Baum, M.; Rieutord, F.; Rebiscoul, D. Underlying Processes Driving the Evolution of Nanoporous Silica in Water and Electrolyte Solutions. *J. Phys. Chem. C* **2020**, *124*, 14531−14540.
(33) Alba-Simionesco, C.; Coasne, B.; Dosseh, G.; Dudziak, G.; Gubbins, K. E.; Radhakrishnan, R.; Sliwinska-Bartkowiak, M. Effects of Confinement on Freezing and Melting. *J. Phys.: Condens. Matter* **2006**, *18*, R15−R68.

https://doi.org/10.1021/acs.jpclett.1c00461
J. Phys. Chem. Lett. 2021, 12, 4038−4044

(34) Morishige, K.; Nobuoka, K. X-Ray Diffraction Studies of Freezing and Melting of Water Confined in a Mesoporous Adsorbent (MCM-41). *J. Chem. Phys.* **1997**, *107*, 6965−6969.
(35) Drebushchak, V. A.; Drebushchak, T. N.; Ogienko, A. G.; Yunoshev, A. S. Crystallization of Sodium Chloride Dihydrate (Hydrohalite). *J. Cryst. Growth* **2019**, *517*, 17−23.
(36) Bee, M. *Quasielastic Neutron Scattering: Principles and Applications in Solid State Chemistry, Biology, and Materials Science*; Adam Hilger: Bristol, 1998; p 28.
(37) Mamontov, E.; Cheng, Y. Q.; Daemen, L. L.; Keum, J. K.; Kolesnikov, A. I.; Pajerowski, D.; Podlesnyak, A.; Ramirez-Cuesta, A. J.; Ryder, M. R.; Stone, M. B. Effect of Hydration on the Molecular Dynamics of Hydroxychloroquine Sulfate. *ACS Omega* **2020**, *5*, 21231−21240.
(38) Chiavazzo, E.; Fasano, M.; Asinari, P.; Decuzzi, P. Scaling Behaviour for the Water Transport in Nanoconfined Geometries. *Nat. Commun.* **2014**, *5*, 3565−11.
(39) Bellissentfunel, M. C.; Chen, S. H.; Zanotti, J. M. Single-Particle Dynamics of Water-Molecules in Confined Space. *Phys. Rev. E: Stat. Phys., Plasmas, Fluids, Relat. Interdiscip. Top.* **1995**, *51*, 4558−4569.
(40) Maruyama, K.; Ohno, S.; Nakada, M. QENS Studies on the Dynamics in Aqueous 1-Propanol Solutions with Kcl. *J. Phys. Soc. Jpn.* **2013**, *82*, SA012−4.
(41) Degreve, L.; Vechi, S. M.; Quintale, C. The Hydration Structure of the Na^+ and K^+ Ions and the Selectivity of Their Ionic Channels. *Biochim. Biophys. Acta, Bioenerg.* **1996**, *1274*, 149−156.
(42) Meyer, A.; Dimeo, R.; Gehring, P.; Neumann, D. The High-Flux Backscattering Spectrometer at the NIST Center for Neutron Research. *Rev. Sci. Instrum.* **2003**, *74*, 2759−2777.
(43) Azuah, R. T.; Kneller, L. R.; Qiu, Y. M.; Tregenna-Piggott, P. L. W.; Brown, C. M.; Copley, J. R. D.; Dimeo, R. M. Dave: A Comprehensive Software Suite for the Reduction, Visualization, and Analysis of Low Energy Neutron Spectroscopic Data. *J. Res. Natl. Inst. Stand. Technol.* **2009**, *114*, 341−358.
(44) Mamontov, E.; Herwig, K. W. A Time-of-Flight Backscattering Spectrometer at the Spallation Neutron Source, Basis. *Rev. Sci. Instrum.* **2011**, *82*, 085109−10.
(45) Arnold, O.; Bilheux, J. C.; Borreguero, J. M.; Buts, A.; Campbell, S. I.; Chapon, L.; Doucet, M.; Draper, N.; Leal, R. F.; Gigg, M. A.; et al. Mantid-Data Analysis and Visualization Package for Neutron Scattering and μ SR Experiments. *Nucl. Instrum. Methods Phys. Res., Sect. A* **2014**, *764*, 156−166.
(46) Mamontov, E.; Smith, R. W.; Billings, J. J.; Ramirez-Cuesta, A. J. Simple Analytical Model for Fitting QENS Data from Liquids. *Phys. B* **2019**, *566*, 50−54.

https://doi.org/10.1021/acs.jpclett.1c00461
J. Phys. Chem. Lett. 2021, 12, 4038−4044